doi:10.1016/j.jmb.2005.02.026 J. Mol. Biol. (2005) 347, 1039–1052

JMB

Available online at www.sciencedirect.com

SCIENCE DIRECT®

ELSEVIER

Structural Dynamics of the DnaK–Peptide Complex

Simone Popp[1], Lars Packschies[2], Nicole Radzwill[3], Klaus Peter Vogel[4] Heinz-Jürgen Steinhoff[4] and Jochen Reinstein[1]*

[1]*Department of Biomolecular Mechanisms Max-Planck-Institute for Medical Research, Jahnstrasse 29, D-69120 Heidelberg Germany*

[2]*Department of Physical Biochemistry Max-Planck-Institut of Molecular Physiology Otto-Hahn-Strasse 11, D-44227 Dortmund, Germany*

[3]*Bruker BioSpin MRI GmbH Rudolf-Planck-Strasse 23 D-76275 Ettlingen, Germany*

[4]*Department of Physics University of Osnabrück Barbarastrasse 7, D-49069 Osnabrück, Germany*

**Corresponding author*

The molecular chaperone DnaK recognizes and binds substrate proteins *via* a stretch of seven amino acid residues that is usually only exposed in unfolded proteins. The binding kinetics are regulated by the nucleotide state of DnaK, which alternates between DnaK·ATP (fast exchange) and DnaK·ADP (slow exchange). These two forms cycle with a rate mainly determined by the ATPase activity of DnaK and nucleotide exchange. The different substrate binding properties of DnaK are mainly attributed to changes of the position and mobility of a helical region in the C-terminal peptide-binding domain, the so-called LID. It closes the peptide-binding pocket and thus makes peptide binding less dynamic in the ADP-bound state, but does not (strongly) interact with peptides directly. Here, we address the question if nucleotide-dependent structural changes may be observed in the peptide-binding region that could also be connected to peptide binding kinetics and more importantly could induce structural changes in peptide stretches using the energy available from ATP hydrolysis. Model peptides containing two cysteine residues at varying positions were derived from the structurally well-documented peptide NRLLLTG and labelled with electron spin sensitive probes. Measurements of distances and mobilities of these spin labels by electron paramagnetic resonance spectroscopy (EPR) of free peptides or peptides bound to the ATP and ADP-state of DnaK, respectively, showed no significant changes of mobility nor distance of the two labels. This indicates that no structural changes that could be sensed by the probes at the position of central leucine residues located in the center of the binding region occur due to different nucleotide states. We conclude from these studies that the ATPase activity of DnaK is not connected to structural changes of the peptide-binding pocket but rather only has an effect on the LID domain or other further remote residues.

Keywords: DnaK; chaperone; mechanism; EPR; structure

Introduction

Hsp70 molecular chaperones are a family of highly conserved ATPases that are present in prokaryotes and in most of the compartments of eukaryotic cells. They are named according to their increased expression under conditions of stress, but are also constitutively expressed and participate in various cellular and regulatory processes.[1–6]

DnaK, the Hsp70 homologue of *Escherichia coli*, consists of two domains: the N-terminal part comprises the nucleotide binding domain (residues 1–388; 44 kDa),[7,8] which binds and hydrolyzes ATP and the C-terminal 26 kDa substrate binding domain, which binds and releases polypeptide targets (residues 389–638).[9,10] The peptide binding domain was found to be composed of two sub-domains: a domain of β-sheet topology that harbours the substrate binding pocket (residues 393–507; 12 kDa) and a 14 kDa domain from residues 508–638, of which the first 100 residues are α-helical. The peptide is bound to DnaK through

Abbreviations used: DTE, dithioerythritol; DnaK and GrpE, DnaK and GrpE from *Escherichia coli*; PEP, phosphoenolpyruvate; PMSF, phenyl methyl sulforyl fluoride; NADH, nicotinamide adenine dinucleotide; ESI-MS, electronspray ionization mass spectroscopy; SL, spin labelled; EPR, electron paramagnetic resonance; MTSSL, (1-oxyl-2,2,5,5-tetramethyl-Δ^3-pyrroline-3-methyl)-methane-thiosulfonate spin label; RT, room temperature; τ, rotational correlation time.

E-mail address of the corresponding author: jochen.reinstein@mpimf-heidelberg.mpg.de

a channel defined by the loops from the β-sandwich, whereas the helical domain appears to act as a moveable LID covering the substrate binding pocket. This LID does not contact the peptide directly, but encapsulates the substrate in the peptide binding channel.[7,11,12]

The main function of DnaK is to facilitate the correct folding of nascent polypeptide chains and denatured proteins.[2,13] Therefore DnaK selectively recognizes and binds to exposed short hydrophobic segments that are primarily flanked by basic residues, while negative charges tend to be excluded throughout.[14,15] In folded proteins these sites are mostly buried in the interior and in the majority are found in β-sheet elements.[15,16]

Efficient folding is then achieved by repeated cycles of binding and release of the substrate from the chaperone. To accomplish that task, DnaK shuttles between an ATP-bound form, which has a low affinity for substrates and therefore binds them with high on and off rates and an ADP-bound form, which has a relatively high affinity for peptides and binds them with slow on and off rates.[17–21] In the ADP-state, the LID is supposed to be predominantly closed. Binding of ATP is thought to shift the equilibrium towards an open conformation in which the LID is assumed to rotate away from the top of the β-sandwich.[9,22]

The switch between the two functional states of DnaK is regulated by the ATPase activity of DnaK and its cochaperones DnaJ (41 kDa; Hsp40) and GrpE (22 kDa).[3,23,24] DnaJ stimulates substrate binding and ATP hydrolysis,[20,25–27] whereas GrpE enhances the exchange of DnaK-bound ADP to ATP.[8,25,28]

Although ATPase and substrate binding activities are divided into separate units, ligand-induced conformational changes appear to be propagated from one domain to the other.[18,19,29,30] Substrate binding stimulates the ATPase activity of DnaK roughly two to tenfold,[20,29,31–34] while ATP binding accelerates peptide exchange by two to three orders of magnitude.[30,35] However, as the structure of the full-length Hsp70/DnaK has not been solved yet, the mechanism of conformational coupling between the two individual domains remains elusive. There is evidence that binding of ATP (and not hydrolysis) causes peptide release[18–20,30,35–37] while ATP hydrolysis mediates the switch back to the tight binding ADP-form.

In addition to this well documented role of ATP hydrolysis the question arises, whether the chemical energy (that is available upon hydrolysis) of ATP is coupled to structural changes of the peptide binding region to also assist peptide release or to result in other properties that mediate correct folding of the substrate protein. Similar to the chaperonin GroE, hydrolysis could thus potentially also drive a "power stroke" that disentangles pre-bound substrate proteins.[38,39] This implies that upon hydrolysis the topology of the peptide binding pocket could be changed such that a bound peptide has to rearrange its structure to accommodate the alternate binding site. In this case the energy of ATP hydrolysis would be used by the chaperone to actively change the conformation of the substrate protein and therefore influence the folding process. Since a corresponding mechanism was actually proposed based on observations of peptide binding and release kinetics,[17,40] it is important to clarify directly if there are corresponding changes of peptide structure concerning the different nucleotide states of DnaK.

To address this question, we performed electron paramagnetic resonance (EPR) measurements with model substrates and monitored their structural and dynamic properties in the presence of different nucleotide states of DnaK (ATP, ADP and nucleotide-free state). To this end we introduced two spin labels at selected positions of peptides using modification of the sulfhydryl group of cysteine residues with a nitroxide reagent.[41,42] Whereas EPR measurements at room temperature (RT) provide information about the mobility of the spin labels, the distance between the two labels can be obtained by low temperature measurements. In combination this information allows the determination of conformational changes in space and time on a millisecond time-scale.[43–45]

We could demonstrate here that the conformation of the model substrates used does not change when bound to different nucleotide forms of DnaK. This indicates that DnaK performs no work on the peptides, which would argue for the chaperone acting solely as a nucleotide-regulated switch that binds and holds onto substrates. Furthermore we could show that changes in the ATPase domain upon binding of ATP are not coupled to parts of the peptide binding site that could be monitored with the EPR spin labels. This suggests that observed changes in peptide exchange dynamics originate from the LID domain and/or other parts of the β-subdomain, but not the central part of the nucleotide binding domain.

Results

Design of suitable peptides

The peptide-binding domain of DnaK from *E. coli* was crystallized previously in the presence of the peptide NRLLLTG[9] that contains the elements of a typical DnaK binding motif: internal hydrophobic residues flanked by terminal polar residues.[15,46] As the position of this peptide in the binding pocket of the chaperone is well defined, we decided to use it as a starting point for EPR measurements. To attach the spin labels to the peptide by site-directed spin labelling, two cysteine residues were added to the C and N-terminal end ($P_{1,9}$, see Table 1) and both were labelled with a (1-oxyl-2,2,5,5-tetramethyl-Δ^3-pyrroline-3-methyl)-methane-thiosulfonate spin label (MTSSL). The advantage of this spin label in general is its relatively small molecular volume, similar in size to a natural tryptophan or

Table 1. Peptides used for EPR measurements

Peptide	Sequence	Name according to position of cysteine residues
P1	**C**NRLLLTG**C**	$P_{1,9}$
P2	**C**NR**C**LLTG	$P_{1,4}$
P3	**C**NRL**C**LTG	$P_{1,5}$
P4	**C**NRLL**C**TG	$P_{1,6}$
P5	Q**RKLFFNLR**KTKQ	–

The modified cysteine residues of the peptides P1–P4 are underlined and highlighted by bold letters. P5 contains the DnaK binding-motif of σ^{32},[58] which is highlighted by bold letters.

phenylalanine sidechain. Therefore it represents only a minimal perturbation of the protein structure, stability and function.[47] While the spin labelled peptide $P_{1,9}$ (SL-$P_{1,9}$) could be used for measurements at room temperature (RT), it was however unsuitable for low temperature distance measurements due to the remoteness of the two labels (data not shown). To reduce the distance between the labels, the sequence of the peptide was modified. As the spin label is hydrophobic, modifications were carried out in the hydrophobic part of the peptide. One cysteine was still attached to the N terminus, but instead of adding a cysteine to the C terminus, each of the leucine residues in the middle of the consensus sequence was replaced by a cysteine. In principle, labelling with MTSSL might lead to sterical hindrance due to the size of the spin label, but it was shown that for example a tryptophan is also well tolerated in the binding pocket of DnaK.[15] The sequences of the peptides used for EPR measurements are summarized in Table 1 ($P_{1,4}$–$P_{1,6}$). Figure 1 shows the respective positions of the cysteine residues in the substrate binding pocket. The cysteine at position 1 sticks out of the peptide binding pocket and points away from the C-terminal domain. Cysteine residues at positions 4 and 6 also stick out of the binding cavity, but they somewhat point towards the LID domain and the loops $L_{3,4}$ (Cys_4) and $L_{1,2}$ (Cys_6), respectively. The cysteine at position 5 is buried in the hydrophobic binding pocket. As spin labels are introduced at four different positions of the peptide, the whole peptide binding pocket is covered evenly, as the mobility at four positions and three different distances can be obtained.

Steady-state kinetics: binding properties of spin labelled peptides

Substrate proteins and peptides stimulate the ATPase activity of DnaK.[34,48] To have a closer look at the binding properties of both unlabelled and spin labelled peptides, DnaK was incubated in the presence of GrpE and ATP with increasing amounts of peptide. The rate of ATP hydrolysis by DnaK was measured in a coupled colorimetric assay at 25 °C (see Materials and Methods) since peptide binding leads to an increased ATPase activity of DnaK.[34] Figure 2 shows the plots of k_{obs} *versus* peptide concentration for unlabelled (a) and labelled (b)

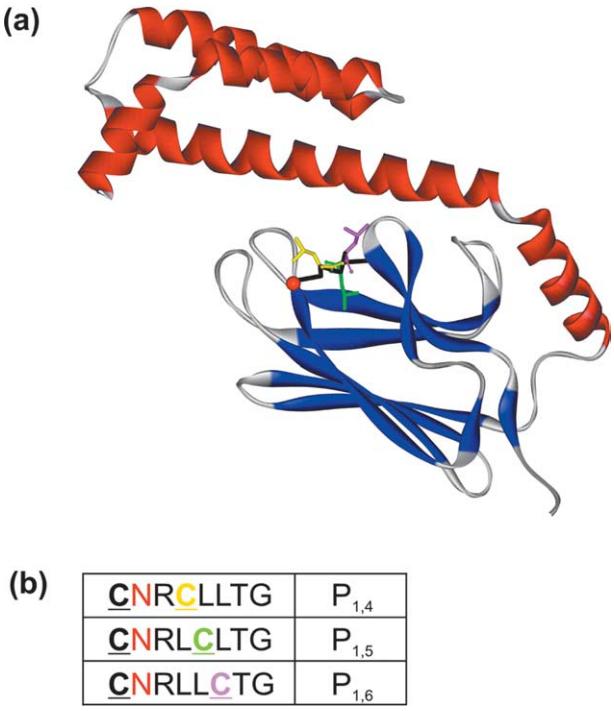

Figure 1. (a) Ribbon diagram of the structure of the substrate binding domain of DnaK in complex with NRLLLTG as determined by X-ray crystallography[9] (PDB1Q5L). β-Strands are shown in blue, whereas α-helices are colored red. The peptide backbone is shown in black together with the respective positions of the cysteine residues in the binding pocket. The cysteine at position 1 is situated one amino acid residue before the N terminus that is marked with a red sphere. The position of cysteine residue 4 is colored yellow, cysteine residue 5 is coded green and cysteine residue 6 is shown in purple. (b) Sequences of peptides used for EPR measurements. Amino acid residues are displayed with the same color code as in (a). Modified cysteine residues are underlined and highlighted by bold letters.

peptides. Analysis of the observed data with the Michaelis–Menten equation gave K_m values in the micromolar range (about 20–40 μM; Table 2) for all unlabelled peptides. $P_{1,5}$ has the highest affinity for DnaK, followed by $P_{1,4}$ and $P_{1,6}$. The presence of the spin labels leads to slightly increased K_m values (30–50 μM). However the k_{cat} values obtained for the ATPase reaction of DnaK when saturated with peptide are equal for labelled and unlabelled peptides (0.6 min^{-1}). An exception is SL-$P_{1,6}$, which yields a slightly lower k_{cat} value but still in the same order of magnitude (0.45 min^{-1}). Hence addition of unlabelled or labelled peptide to DnaK·ATP leads to an approximately fourfold acceleration of ATP hydrolysis at saturating peptide concentrations.

As a reference we also measured the binding properties of the unmodified peptide NRLLLTG (data not shown). The obtained K_m value is around 20 μM. Therefore it is in the range of the modified, unlabelled peptides (Table 2), as is the k_{cat} value

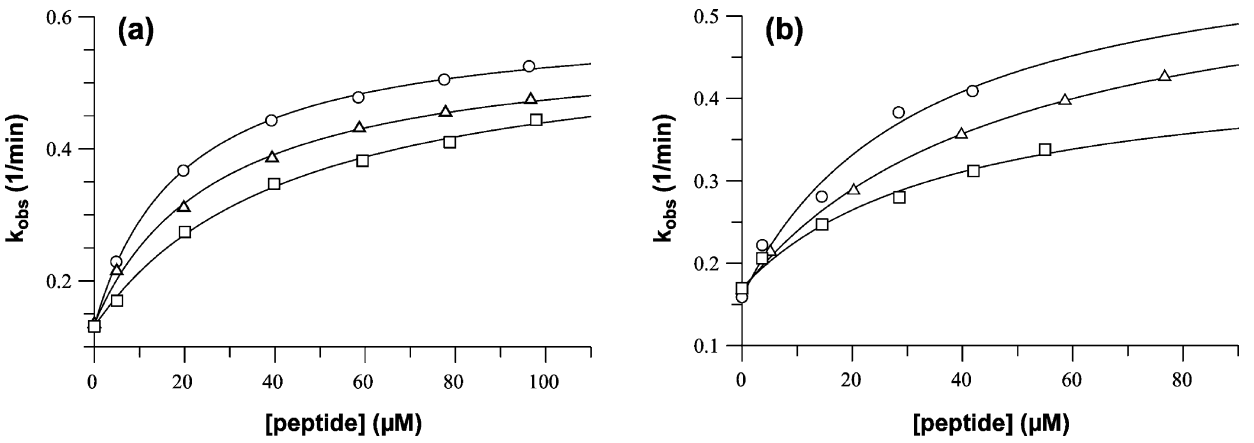

Figure 2. Steady-state analysis of ATP hydrolysis by DnaK in the presence of GrpE and unlabelled (a) or labelled (b) peptide. The observed turnover numbers for ATP hydrolysis at 25 °C were determined with a coupled colorimetric steady-state assay as described in Materials and Methods. 10 μM DnaK and 0.1 μM GrpE were incubated with various amounts of peptide in NADH buffer (△, $P_{1,4}$ or SL-$P_{1,4}$; ○, $P_{1,5}$ or SL-$P_{1,5}$; □, $P_{1,6}$ or SL-$P_{1,6}$). The obtained data for ATP hydrolysis were fitted to the Michaelis–Menten equation. Corresponding K_m and k_{cat} values are listed in Table 2.

(0.6 min^{-1}) and ATPase-stimulation factor (×4). This clearly demonstrates that modification of the peptide with cysteine residues, regardless of their position, does not considerably alter their binding properties. In addition, labelling of the modified peptides with MTSSL does not disturb the binding of the peptides to DnaK. As the kinetic properties concerning ATPase-stimulation are also comparable, they were considered suitable peptide probes for EPR measurements.

Low temperature EPR measurements: distance of spin labels

The spin–spin interaction between two spin labels attached to a peptide is composed of static dipolar interaction, modulation of the dipolar interaction by the rotational diffusion of the peptide and residual motion of the spin label side-chains as well as exchange interaction. In the frozen state (temperatures below 200 K) dynamic effects, including the rotational diffusion and the residual motion are strongly restricted.[49] Static dipolar interaction leads to broadening of the spectrum. An analysis of the line shape allows the determination of inter-spin distances.[50–54] Thus, information on conformational changes of the molecule can be obtained with limitation of quantitative analysis to inter-spin distances within the range of 1.0–2.5 nm.[52,55]

EPR spectra of free spin labelled peptide and peptide in complex with DnaK (in the nucleotide-free, ADP and ATP-form, respectively) were measured at 170 K in frozen solution to exclude protein fluctuations and motional averaging of the dipolar broadening of the spectra. To obtain the absolute values of the inter-spin distances, simulated powder spectra were fitted to the experimental data using the method described by Steinhoff *et al*.[52] (see Materials and Methods).

Figure 3(a) shows a comparison of the spectra of the spin labelled peptides, which were normalized to a constant spin number. The extracted inter-spin distances are summarized in Table 3. The average inter-spin distance of all three free peptides is around 1.9 nm, which means that they are likely to appear in an extended conformation. The experimental data could be quite well simulated by powder spectra (Figure 3(b)–(d)). In the case of SL-$P_{1,4}$, addition of nucleotide-free DnaK exhibits a broadening of the line width and consequently a smaller amplitude due to increased dipolar interaction (Figure 4(a)). This indicates a decrease in the inter-spin distance that can be confirmed with the calculated value of 1.7 nm (Table 3). For SL-$P_{1,5}$, addition of DnaK leads to only slight changes of the shape of the spectra (data not shown), which is consistent with the obtained distance of 2.0 nm compared to 1.8 nm for the free peptide. In the presence of DnaK, the calculated inter-spin distance

Table 2. Influence of labelled and unlabelled peptides on DnaK mediated ATP hydrolysis

	K_m (μM)		k_{cat} (min^{-1})		ATPase-stimulation factor	
Peptide	Unlabelled	Labelled	Unlabelled	Labelled	Unlabelled	Labelled
$P_{1,4}$	27.1 (±2.8)	48.8 (±4.8)	0.57 (±0.02)	0.59 (±0.02)	4.2	3.5
$P_{1,5}$	19.4 (±0.8)	32.2 (±17)	0.60 (±0.01)	0.61 (±0.12)	4.5	3.8
$P_{1,6}$	44.0 (±4.7)	38.4 (±12.7)	0.58 (±0.02)	0.45 (±0.05)	4.4	2.6

K_m and k_{cat} values as well as ATPase-stimulation factors were compared for the labelled and unlabelled peptides with a steady-state ATPase assay as described in Materials and Methods.

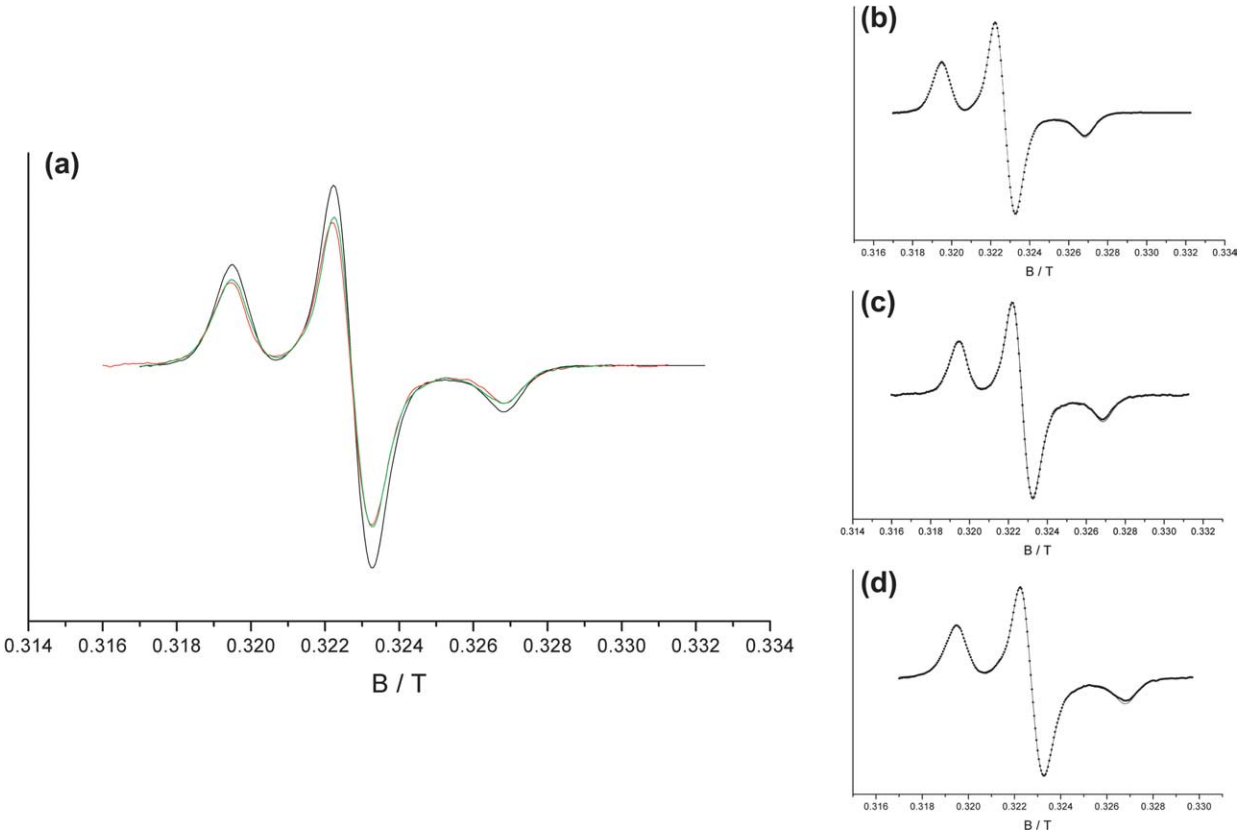

Figure 3. (a) EPR spectra of free spin labelled peptides determined at 170 K. The spectra were normalized to a constant spin number. SL-$P_{1,4}$ is shown in black, SL-$P_{1,5}$ in red and SL-$P_{1,6}$ in green. (b)–(d) EPR spectra of SL-$P_{1,4}$–SL-$P_{1,6}$ compared to the simulated powder spectra:[52] (···) experimental data, (—) fit (see Materials and Methods).

between the two labels of SL-$P_{1,6}$ considerably increases from 1.8 nm to >2.3 nm. It is also interesting to note that, in the presence of DnaK, the inter-spin distance increases with increasing distance between the labelled cysteine residues.

The same inter-spin interactions and distances were obtained when DnaK in the ADP-bound state was added to the labelled peptides (Figure 4(a) and Table 3).

As dipolar interaction was detectable for all peptides in the presence of nucleotide-free DnaK or DnaK·ADP, these peptides appear to be suitable to address the question, of whether addition of DnaK·ATP could result in an altered conformation of the peptides relative to the DnaK·ADP complex. This would lead to different spin–spin interactions compared to nucleotide-free or ADP-bound DnaK, which should in turn be detectable in the shape of the spectra. To test this, ATP was added to DnaK and peptide. However, EPR spectra in the presence of ATP exhibit a similar line shape, indicating a similar distance between the two labels for the three DnaK forms. Simulation of powder spectra gave the same result (Table 3). For all peptides the binding of the peptide to DnaK leads to changes in the inter-spin distance, but no further significant changes in the inter-spin distance could be measured with different forms of DnaK (nucleotide-free, with ADP or with ATP). The fitted powder spectra of the EPR measurements of SL-$P_{1,4}$ at low temperature are shown in Figure 4(b)–(d). For all peptides and complexes measured the statistical error of the calculated distances amounts to less than 0.1 nm.

Table 3. Inter-spin distances of spin labelled peptides in nm

	SL-$P_{1,4}$	SL-$P_{1,5}$	SL-$P_{1,6}$
SL-P	2.0	1.8	1.8
SL-P + DnaK	1.7	2.0	>2.3
SL-P + DnaK + ADP	1.6	2.0	2.2
SL-P + DnaK + ATP	1.6	2.1	2.3

Powder spectra simulations were fitted to the experimental data. Values for the average distances were obtained for free peptides, peptides in the presence of nucleotide-free DnaK, DnaK + ADP and DnaK + ATP. The distance distribution width was fixed to 0.45 nm for all simulations. Statistical errors of the distance values were less than 0.1 nm.

Room temperature EPR measurements: mobility of spin labels

Room temperature measurements were performed to characterize the side-chain mobility of the spin labels to obtain information on the dynamics of the molecule and the local environment around the labels. At RT the correlation time of the spin label side-chain motion is in the

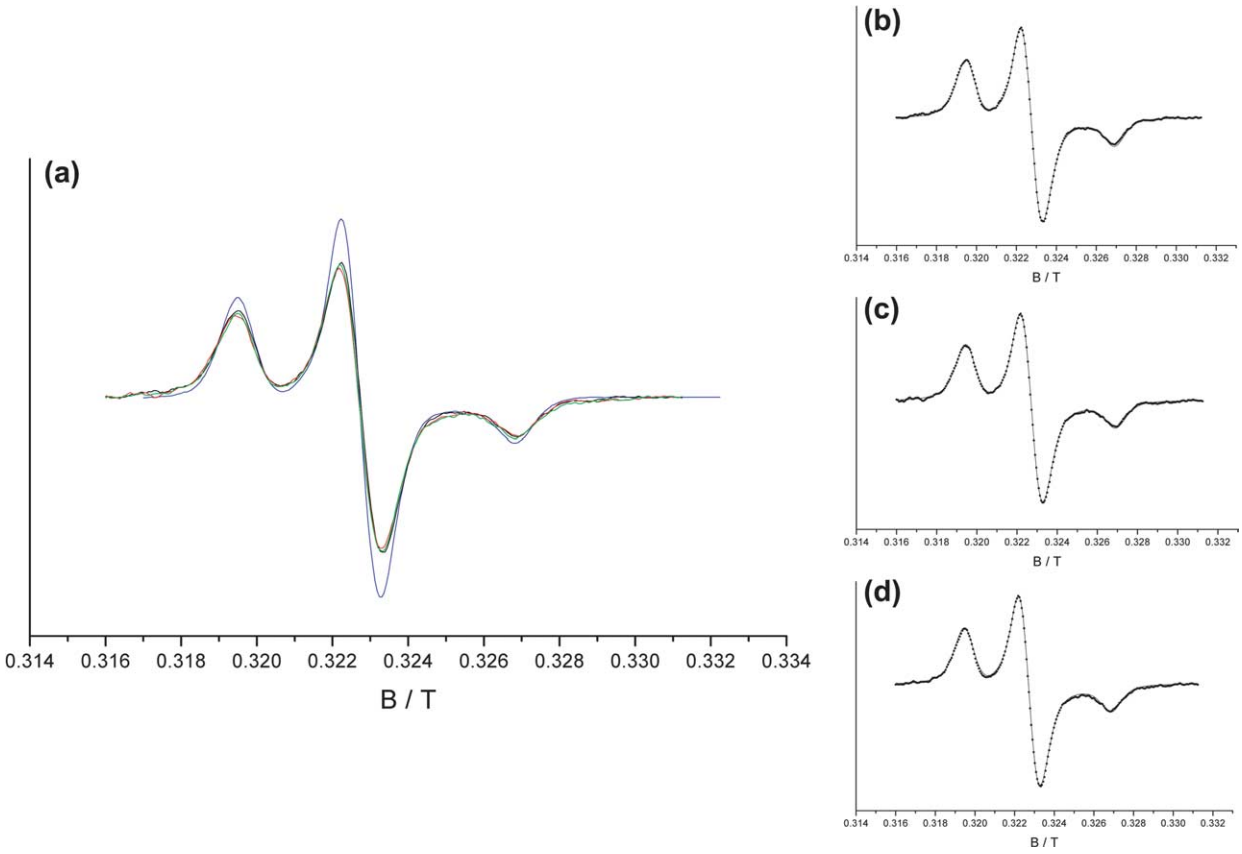

Figure 4. Binding of SL-$P_{1,4}$ to DnaK measured by low temperature EPR spectroscopy. (a) EPR spectra of free SL-$P_{1,4}$ (blue) and in the presence of DnaK (black), DnaK + ADP (red) and DnaK + ATP (green) at 170 K. The spectra were normalized to a constant spin number. (b)–(d) EPR spectra compared to simulated powder spectra: (⋯) experimental data, (—) fit. (b) SL-$P_{1,4}$ + DnaK, (c) SL-$P_{1,4}$ + DnaK + ADP, (d) SL-$P_{1,4}$ + DnaK + ATP.

nanoseconds time range, and the mobility of the nitroxide group as well as the flexibility of its binding site are directly reflected in the EPR absorption line shape.

Figure 5 shows the EPR spectra of the free spin labelled peptides, which were normalized to a constant spin number. The line shape of the spectra exhibits a typical line broadening due to the restriction of the nitroxide reorientational motion that occurs upon covalent binding of the spin label.

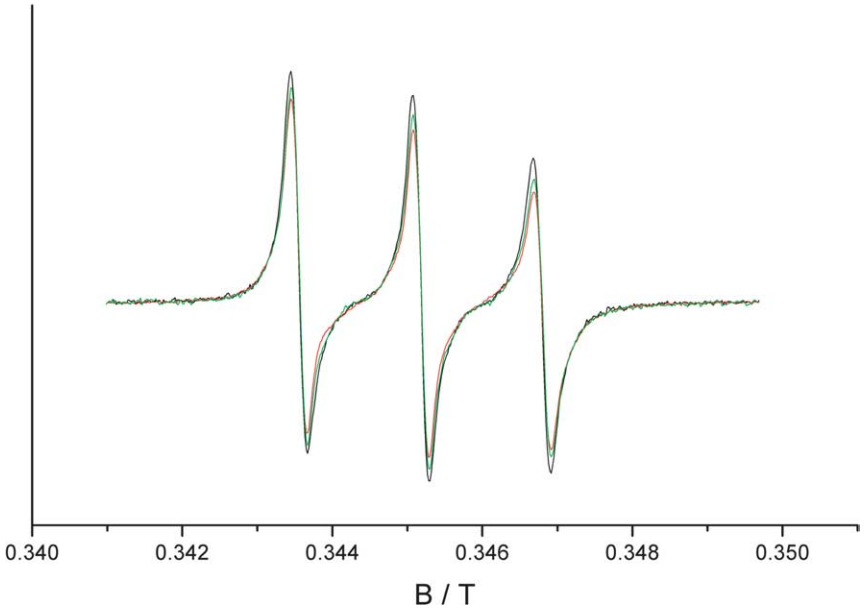

Figure 5. Room temperature spectra of the spin labelled peptides. The spectra were normalized to a constant spin number. SL-$P_{1,4}$ is shown in black, SL-$P_{1,5}$ in red and SL-$P_{1,6}$ in green.

Furthermore the spectral shape is characteristic for short-range Heisenberg interactions. Those appear when the molecules in solution can adopt a conformation with a short distance between the labels (<1 nm), which leads to strong interactions of the unpaired electron spins of the two nitroxides.

Upon binding of the spin labelled peptides to DnaK, the Heisenberg interactions are completely diminished, which leads to considerable changes in the line shape. Those differences can be observed most clearly from the ratio of the amplitudes of the peaks and typical changes at the peak base of the recorded spectra as shown exemplary for SL-$P_{1,4}$ (Figure 6(a)).

As the spectral shape exhibits two components of different spin label mobility, the experimental data were analyzed allowing two different rotational correlation times assuming a Brownian diffusion model.[56] Double integration of the two simulated curves defines the contribution of the components to the measured EPR spectra, as the area of the absorption spectrum is directly proportional to the number of spins. The determined rotational correlation times (τ) and the contribution of the respective components to the spectra are summarized in Table 4. For all spin labelled peptides in the presence of nucleotide-free DnaK, the τ value for the mobile component is close to 0.15 ns and close to 4 ns for the more immobile component. The mobile component accounts for 30–50% of the area of the measured spectra.

Addition of DnaK·ADP indicates that the mobility of the spin labels is not significantly altered. There are no spectral changes at the peak base and only a slight decrease at the top of the peak, which is confirmed by the nearly unchanged τ values and areas of the associated components (Figure 6(a) and Table 4).

A slightly different picture emerges when ATP-bound DnaK was added to the peptide (Figure 6(a)). The spectra reveal an increased contribution of the mobile component for all peptides by 20% upon addition of ATP in comparison to the ADP-bound state (Table 4). Although error analysis indicates that this change is significant in relation to the errors obtained ($\pm$5% to 14%), overall the rotational correlation times have to be considered similar for the different DnaK-states. Thus changes in the contribution of the mobile component to the measured spectra are too minor to be associated to changes in the conformation of the peptide. Differences of the spectral shape occur probably only due to different peptide binding properties of DnaK in the presence of ADP and ATP. In the ATP-bound form, the LID is thought to be

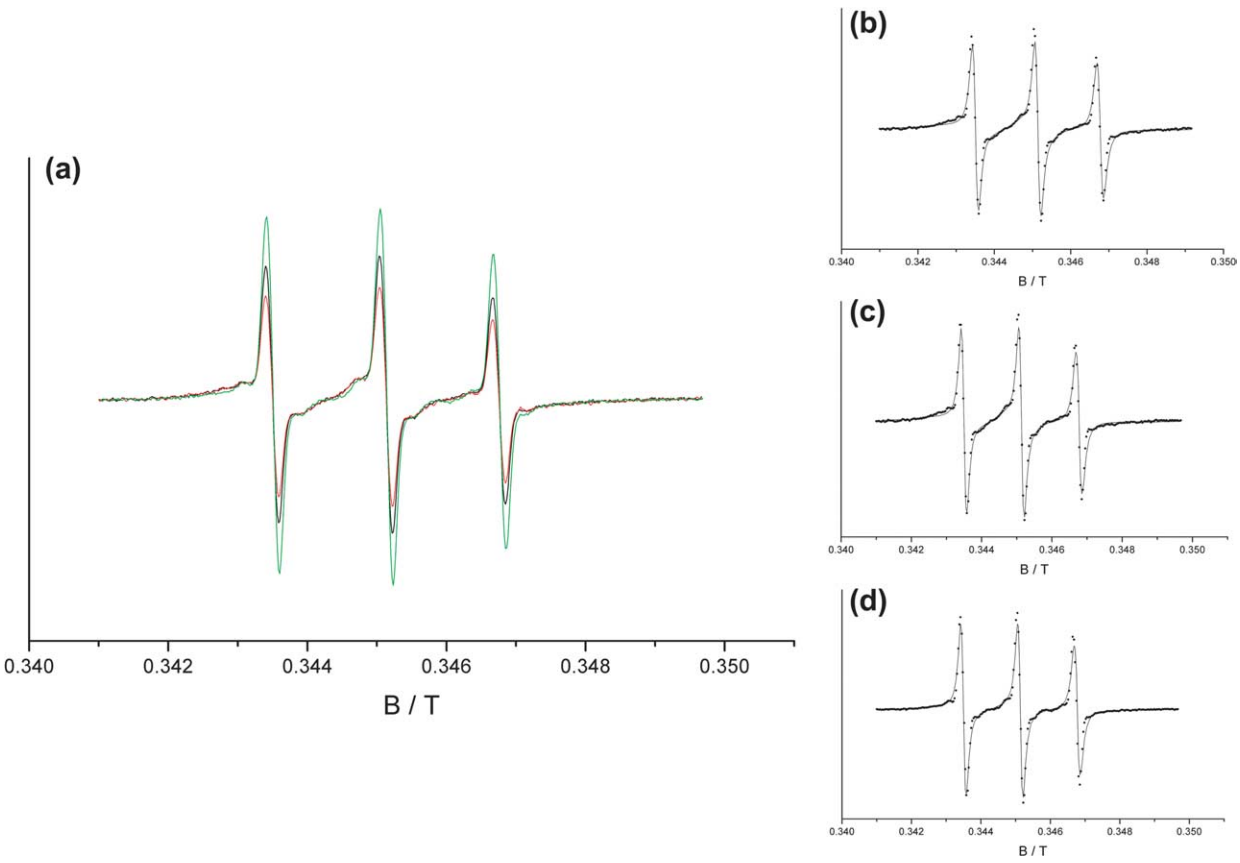

Figure 6. Binding of SL-$P_{1,4}$ to DnaK measured by room temperature EPR spectroscopy. (a) EPR spectra of SL-$P_{1,4}$ + DnaK (black), SL-$P_{1,4}$ + DnaK + ADP (red) and SL-$P_{1,4}$ + DnaK + ATP (green). The spectra were normalized to a constant spin number. (b)–(d) EPR spectra compared to simulated spectra according to the Brownian diffusion model:[56] (···) experimental data, (—) fit. (b) SL-$P_{1,4}$ + DnaK, (c) SL-$P_{1,4}$ + DnaK + ADP, (d) SL-$P_{1,4}$ + DnaK + ATP.

Table 4. Rotational correlation times τ and contribution of the respective component to the measured spectra

Peptide	Nucleotide	τ_{mobile} (ns)	$\tau_{immobile}$ (ns)	Area mobile component (%)
SL-$P_{1,4}$	–	0.10±0.02	3.5±0.9	42±6
SL-$P_{1,4}$	ADP	0.10±0.02	3.5±0.9	33±7
SL-$P_{1,4}$	ATP	0.10±0.02	3.5±0.8	57±13
SL-$P_{1,5}$	–	0.13±0.03	3.7±0.9	29±6
SL-$P_{1,5}$	ADP	0.13±0.03	3.7±0.4	24±5
SL-$P_{1,5}$	ATP	0.10±0.03	3.3±0.8	51±10
SL-$P_{1,6}$	–	0.17±0.02	3.6±0.9	48±9
SL-$P_{1,6}$	ADP	0.18±0.02	3.3±0.4	39±4
SL-$P_{1,6}$	ATP	0.11±0.03	5.6±1.4	59±14

Values were obtained through analysis of the experimental data using the Brownian diffusion model.[56] Values were obtained for spin labelled peptides in the presence of nucleotide-free DnaK, DnaK + ADP and DnaK + ATP.

predominantly open, which leads to a better accessibility of the peptide binding channel and allows rapid diffusion of the peptide into the binding crevice.[9,57] The simulated spectra for SL-$P_{1,4}$·DnaK according to the Brownian diffusion model are shown in Figure 6(b)–(d). Also in the case of measurements at RT the experimental data could be described well considering that the assumption of isotropic spin distributions does not exactly hold for peptides bound to DnaK.

Control: displacement by unlabelled peptide

It was shown that the shape of the room temperature EPR spectra considerably changes when DnaK is added to the peptide. To make sure that the differences are not due to changes in the viscosity of the solution or due to dimerization of free label, we tried to displace the spin labelled peptides by a non-labelled peptide and measured the EPR spectra again. If SL-dimers occur in the solution, they cannot bind to DnaK and therefore cannot be displaced by a non-labelled peptide. In this case the spectra will not change their shape. If incubation with the unlabelled peptide affects the line shape, one can ascertain that the labelled peptide was previously bound to DnaK. It is important to note that the unlabelled peptide must not contain a cysteine, because the spin label can be passed over to the free SH-group. In this case single-labelled peptides would occur leading to a loss of intramolecular spin interactions.

To carry out this experiment, we used the peptide P5, which includes the constitutive binding site for DnaK, RKLFFNLR, in the regulatory region C of the heat shock transcription factor σ^{32} (AA 133–145, Table 1,[58]). Steady-state kinetic analysis of ATP hydrolysis by DnaK in the presence of P5 gave a K_m value of 19.2 μM (data not shown). Hence the peptide can be used for displacement, because it binds with a higher affinity to DnaK than the spin labelled peptides (Table 2). Furthermore the obtained k_{cat} value of 0.58 min^{-1} and the ATPase stimulation factor of 4.2 are in the range of the obtained values for the other peptides. For all three peptides it could be shown that an excess of P5 can displace the SL-peptide from a preformed SL-P·DnaK complex (data not shown).

Discussion

The aim of this work was to elucidate the potential role of ATP hydrolysis in the functional cycle of DnaK beyond the known modulation of the LID domain that regulates nucleotide access. In the latter case, the two different nucleotide states (ADP *versus* ATP) would merely constitute a switch that drives the alternating high affinity/slow exchange (ADP; holding) and moderate affinity/fast exchange (ATP; folding) states, indicating that DnaK functions *via* a mostly passive holdase activity.[16] An extended model considers that DnaK may influence the folding process with a so-called power stroke or catapult mechanism.[17,40,59–61] In this case DnaK would act as an unfoldase that actively changes the conformation of substrate proteins by repeatedly binding and pulling apart the substrate protein, which has been referred to as "plucking".[62]

With EPR measurements at low temperature it could be clearly demonstrated that only the binding of free peptide to DnaK leads to changes in the distance between the spin labels, which means that the conformation of the bound peptide is distinct from the conformational average of the free peptide. Interestingly, the inter-spin distance does not significantly change upon addition of ADP or ATP to the DnaK·peptide-complex (Table 3). These results indicate that the structure of the peptide is already determined *via* its binding to DnaK and that there are no additional conformational changes of the peptide, regardless of the nucleotide state of DnaK.

Furthermore it could be observed that the spin–spin interaction decreases with increasing distance between the labelled cysteine residues when the peptide is bound to DnaK (Table 3). From X-ray and NMR experiments it is known that the peptide is bound in an extended conformation in the binding cavity of the peptide binding domain of DnaK through a channel defined by the loops of the β-sandwich, whereof two loops form the channel directly and the other two loops stabilize the

channel.[9,63,64] In this conformation the average distance between C^{α} atoms of two adjacent amino acid residues is 0.34 nm. Therefore the calculated distance between the cysteine residues of the three peptides is 1.02 nm for SL-$P_{1,4}$, 1.36 nm for SL-$P_{1,5}$ and 1.7 nm for SL-$P_{1,6}$ (Figure 7). For each peptide the measured distance does not correspond to the C^{α} distance but is always 0.6–0.7 nm larger than the calculated data. Hence our results agree very well with the theoretical distances for model peptides in an extended conformation, because one has to consider that the label is not directly situated at the C^{α} atom but has a side-chain length of approximately 0.7 nm and that the orientation of the two labels is restricted due to steric hindrance. Thus it could be shown that the peptide NRLLLTG is also bound in an extended conformation to the holoenzyme.

The conformational change of the peptide upon binding to DnaK could be confirmed with EPR measurements at RT. In the case of the free spin labelled peptides, Heisenberg interactions can be observed due to the potentially short distance between the labels. When the peptides are bound to DnaK those interactions are completely diminished, because the spin labels are no longer at close quarters (Figures 5 and 6).

Moreover, interpretation of the data at RT gave two components with different rotational correlation times (Table 4). One explanation could be that the part with the higher mobility accounts for the unbound spin labelled peptide, which would mean that 30–50% of the peptide is existing in the unbound form in the case of nucleotide-free or ADP-bound DnaK. But this is in conflict with the obtained affinity of the peptides for DnaK (Table 2) and the resultant concentrations of DnaK and peptide that were used in our experiments (Materials and Methods; at most 10–14% should be free). Besides, the presence of 50% free spin labelled peptide would obviously change the spectral shape due to the reappearing Heisenberg interactions, which rules out this possibility. Thus, the two components must appear due to the different mobility of the two spin labels. It is difficult to determine which of the labels is the one with the higher mobility. As the structure of the full-length DnaK is not known, there is no information available about the local environment of the spin label attached to the cysteine residue at the N terminus and the interaction of this spin label with the ATPase domain cannot be predicted. It was deduced from X-ray and NMR studies that there is a differential immobilization of the peptide backbone compared to the side-chains in complex with DnaK. Between the side-chains of the three leucine residues and the β-subdomain of DnaK only some weak interactions occur, whereas seven stable hydrogen bonds are formed between the main chain of the peptide and the binding cavity.[9,64] Therefore it is very likely that the peptide backbone has a greater participation in the interaction with DnaK. This could explain why both labels are still very mobile, as they are attached to the side-chains of cysteine residues. The NMR structure of the β-subdomain in complex with the peptide shows that NRLLLTG is much more flexible at the N terminus in contrast to the middle of the peptide, which is relatively rigid.[64] This finding is supported by the crystal structure that also indicates an increased mobility of the peptide termini.[9] Therefore it is tempting to speculate that the more mobile label is situated at the N-terminal cysteine.

The EPR experiments at RT also suggest that the mobility of the spin labels does not significantly change in the presence of different forms of DnaK, as the rotational correlation time stays quite the same for all peptides (Table 4). This indicates as well that the local environment of the spin labels is not altered and that the monitored part of the binding cavity does not change its conformation upon binding of ADP or ATP to the substrate-binding domain, which is in accordance with the measurements at low temperature. There are in fact some changes upon the addition of ATP-bound DnaK to the peptides, as the contribution of the mobile component increases around 20% in comparison to the ADP-bound state (Table 4). We attribute this change mainly to the fact that the ADP and ATP-state of DnaK differ in their frequency of conformational changes that cause opening of the substrate binding cavity rather than to changes in

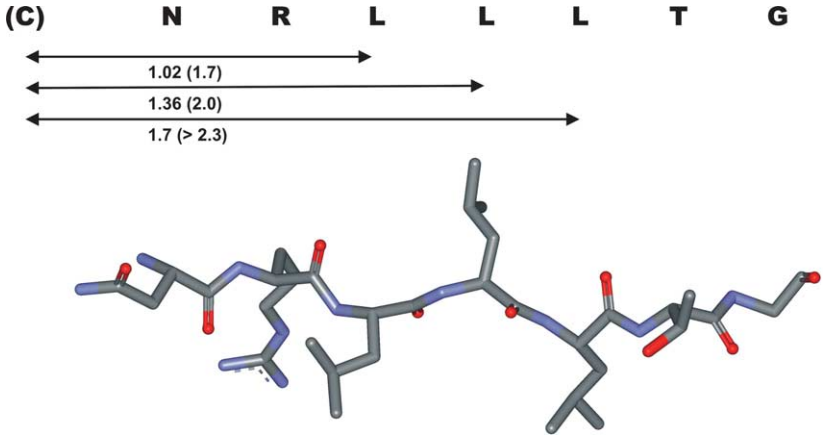

Figure 7. Sequence and structure of the peptide NRLLLTG. (C) indicates the N-terminal cysteine residue. The values describe the theoretical distances between the C^{α} atoms of the leucine (replaced by cysteine) residues (depicted with arrows) assuming an extended conformation of the peptide. The values in brackets correspond to the experimental obtained distances of the spin labels attached to cysteine residues. All distances are given in nm.

peptide conformation. In the ADP-state the LID is supposed to be predominantly closed, whereas it is thought to be predominantly open in the ATP-state.[9] This leads to a better accessibility of the binding pocket and accelerates peptide exchange, which in turn accounts for the observed changes in the shape of the EPR spectra. The contribution of the mobile component in the case of the peptide bound to nucleotide-free DnaK lies in between the ADP and the ATP-state of DnaK, but closer to the ADP-state (Table 4).

Taken together these results strongly suggest that DnaK performs no work on the peptides, as the mobility of the labels and the distance between them virtually stays the same when different forms of DnaK are added. This implies that DnaK acts more like a holdase than a foldase, since only the exchange rate of the peptides is affected and not their conformation. We therefore conclude that changes in the ATPase domain upon binding and hydrolysis of ATP are not associated with the part of the peptide binding site that could be monitored by the spin labels of the peptides, as the structure of these is not affected. Consequently, we propose that the monitored part of the peptide binding pocket possesses a rigid structure and that changes that couple the ATPase activity of DnaK to peptide binding must originate mostly from the LID and/or other parts of the β-subdomain without affecting the peptide structure.

Our data are consistent with the findings of recent studies that revealed that the LID, especially the helical elements αA and the first half of αB are required for domain–domain-coupling.[65,66] In addition, it was reported that the α-helical domain is also responsible for interdomain-interaction and that the LID and the β-sandwich together facilitate peptide binding to DnaK.[22,57,66,67] It was also suggested that the C-terminal end of strand β3 and the remote loop $L_{2,3}$ of the β-subdomain are important for the allosteric regulation of substrate binding by the nucleotide binding domain.[30,67–70] Other experiments could show that the allosteric interface[25,30,35,71–74] and the highly conserved linker group[27,48,70] between the two domains are jointly responsible for interdomain communication. All these proposed positions of domain–domain communication lay mostly outside the peptide binding region and consistently could not be monitored with the spin labels reported here. The final conclusion that has to be reached is that at least DnaK alone does not couple ATPase activity to structural changes of bound peptide that could introduce asymmetry in peptide binding or be related to active transport and folding processes.

Materials and Methods

Materials

ATP and ADP (disodium salt) were purchased from Pharma Waldhof Mannheim. Tris (ultrapure), NADH and PEP were purchased from Roche Diagnostics Mannheim and $MgCl_2 \cdot 6H_2O$ from Aldrich. KCl, NaCl, PMSF and EDTA were purchased from Fluka and DTE from Gerbu.

Recombinant nucleotide-free DnaK from *E. coli* was prepared as described.[36] For EPR measurements, the protein was dialyzed against EPR buffer (50 mM Tris–HCl (pH 7.5), 100 mM KCl, 5 mM $MgCl_2$, 2 mM EDTA) in order to remove DTE. Recombinant GrpE from *E. coli* was purified as described.[28] Concentrations of both proteins were determined photometrically by the method described by Ehresmann.[75]

Synthesis and spin labelling of peptides

Peptides P1 and P5 (Table 1) were generously provided by R. Frank (ZMBH Heidelberg). Peptides P2–P4 were synthesized by solid phase peptide synthesis[76] by S. Gentz (MPI Dortmund), applying the Boc-protection strategy.[77] For Boc-group removal the peptides were treated with HF and *p*-cresol. Peptides were purified by reverse-phase chromatography with a Prontosil-C18 column (250 mm × 20 mm; Bischoff). They were eluted with an acetonitrile gradient and identified by ESI-MS. The peptide-containing fractions were lyophilized and stored at −80 °C.

To covalently link the spin label to the peptide, 1 mg peptide was incubated with 30 μl of 100 mM MTSSL in 500 μl of acetonitrile and 270 μl of H_2O. After 16–24 hours at 30 °C overnight (in the dark), the reaction mixture was loaded onto an ODS-Hypersil-column (250 mm × 8 mm; Bischoff). Excess spin label as well as unlabelled peptide were removed at RT by reverse-phase chromatography with a linear gradient of 33% to 75% acetonitrile (v/v) in 0.17% triflouroacetic acid (v/v). Spin labelled peptide was subsequently identified by ESI-MS. The pooled fractions were lyophilized twice and dissolved in a small amount of water. Finally, samples were shock frozen in liquid nitrogen and stored at −80 °C.

The concentration of the peptides was obtained from double integration of the EPR spectra by comparison with those of a standard solution of free spin label (TEMPO = 2,2,6,6-tetramethyl-1-piperidin-1-oxyl) that was analyzed under the same conditions.

Steady-state kinetics

Steady-state ATP hydrolysis by DnaK in the presence of GrpE and unlabelled or spin labelled peptide was measured in a coupled colorimetric assay.[78] Addition of catalytic amounts of GrpE assures that DnaK is predominantly in the ATP-state even if peptide stimulates ATP hydrolysis. 10 μM DnaK, 0.1 μM GrpE and 1 mM ATP were incubated at 25 °C with various concentrations of peptide in 50 mM Tris–HCl (pH 7.5), 100 mM KCl, 5 mM $MgCl_2$, 2 mM EDTA, 0.4 mM PEP, 0.2 mM NADH with 25 μg ml^{-1} lactate dehydrogenase (Roche Diagnostics, Mannheim) and 62.5 μg ml^{-1} pyruvate kinase (Roche Diagnostics, Mannheim) (NADH buffer). 2 mM DTE was added for the measurements with unlabelled peptides to avoid covalent dimerization. The observed turnover number (k_{cat}) for ATP hydrolysis was determined from the decrease of A_{340} due to the oxidation of NADH. Data were fitted to the Michaelis–Menten equation with offset, where Δv_{stim} is the increase of ATPase activity upon stimulation by peptide and v_0 is the intrinsic ATPase activity:

$$v = \Delta v_{\text{stim}} \frac{S}{K_m + S} + v_0$$

EPR measurements

EPR measurements were carried out using home-made X-band spectrometers equipped with a dielectric resonator (RT, ER4118X-MD5, Bruker, Gemany) or with a H_{103} rectangular cavity (AEG, Germany). For low temperature experiments a modified Oxford ESR 9 variable temperature accessory stabilized the sample temperature at 170 K. The magnetic field was measured with B-NM 12 B-field meter (Bruker). Spectra were recorded with modulation amplitudes of 0.25 mT (low temperature) or 0.2 mT (RT) and a microwave power adjusted to between 0.1 mW and 0.6 mW. After analog to 12 bit digital conversion the data were processed in a PC.

All measurements were performed in EPR buffer (50 mM Tris–HCl (pH 7.5), 100 mM KCl, 5 mM $MgCl_2$, 2 mM EDTA). The final concentration for free spin labelled peptide was 50 μM at RT and 80 μM at 170 K. All samples contained 320 μM chaperone, 30 μM spin labelled peptide, 1 μM GrpE and 62.5 μg ml^{-1} pyruvate kinase. In addition, for measurements with ADP-bound DnaK, 1 mM ADP was added or 5 mM PEP and 10 mM Mg·ATP in the case of ATP-bound DnaK. For measurements at low temperature, 30% glycerol was added to the prepared samples to prevent precipitation. With glycerol the peptides remained soluble during the freezing process and the average inter-spin distances could be measured (see Figure 3 and Table 3). The same effect and the same distances can also be obtained with only 10% or 20% glycerol (data not shown). To show that glycerol has no effect on the conformation of the peptide, the same experiment was carried out at RT. The peptide was investigated in the absence of glycerol and in the presence of 10% or 30% glycerol (data not shown). The observed spectral changes can be attributed only to increasing viscosity of the solution.

All samples were incubated for 30 minutes at RT, before they were transferred to EPR quartz capillaries (10 μl for measurements at RT, otherwise 60 μl).

To examine whether the spin labelled peptide can be displaced by an excess of unlabelled peptide, 10 μl of the nucleotide-free DnaK sample including the spin labelled peptide, GrpE and pyruvate kinase (incubated for one hour at RT) were mixed with 600 μM P5 and incubated for another 30 minutes before loading into the capillary.

Spectra were averaged by recording five to eight scans that were normalized to a constant spin number. Fitting of simulated dipolar broadened EPR powder spectra to the experimental data of doubly spin labelled samples were performed using the method described recently by Steinhoff *et al*.[52] Due to the flexible spin label side-chain a random distribution of nitroxide ring orientations with respect to the inter-spin vector is assumed. To account for a range of distances expected to arise from these different orientations, a Gaussian distribution of inter-spin distances with fixed width of 0.45 nm is permitted. During the fitting procedure the g-tensor values, two components of the A-tensor and the line width parameters were fixed according to the values given by Tiebel *et al*.[79] The agreement between simulation and experimental data could be further improved by the use of a slightly lower value of g_{xx} according to the data of MTSSL in polar environment.[80] The values finally used are: $g_{xx}=2.0084$, $g_{yy}=2.0065$, $g_{zz}=2.0026$, $A_{xx}=0.54$ mT, $A_{yy}=0.49$ mT. A_{zz} was kept variable to account for a possible polarity variation in the vicinity of the nitroxides. The spectra were convoluted with a field-independent line shape function, composed of a superposition of 53% Lorentzian and 47% Gaussian of 0.48 mT and 0.41 mT width, respectively. The list of fitting parameters is thus composed of the average inter-spin distance, the fraction of singly labelled peptide and A_{zz}.

At RT the spectra of the peptide in the presence of DnaK were analyzed according to the Brownian model of isotropic reorientational diffusion.[56] Assuming two components contributing to the spectra, one reflecting the more mobile spin label of the peptide and one representing the rather immobile spin label, the simulations are in good agreement with the measured spectra. Variable parameters during the fitting procedure are the spin-lattice relaxation time and the reorientational diffusion time for each component as well as the ratio of the two components.

Acknowledgements

This work was supported by a grant of the Deutsche Forschungsgemeinschaft to J.R. (SFB 394, RE 1212/1-1) and H.-J.S. (SFB 394, STE 640/5). We are indebted to Ilme Schlichting and Roger S. Goody for continuous and generous support, Ralf Seidel for help with the peptide synthesis and Bernd Bukau for kindly supplying a DnaK over-expressing plasmid.

References

1. Gething, M. J. & Sambrook, J. (1992). Protein folding in the cell. *Nature*, **355**, 33–45.
2. Craig, E. A., Gambill, B. D. & Nelson, R. J. (1993). Heat-Shock Proteins—Molecular Chaperones of Protein Biogenesis. *Microbiol. Rev.* **57**, 402–414.
3. Bukau, B. & Horwich, A. L. (1998). The Hsp70 and Hsp60 chaperone machines. *Cell*, **92**, 351–366.
4. Netzer, W. J. & Hartl, F. U. (1998). Protein folding in the cytosol—chaperonin-dependent and -independent mechanisms. *Trends Biochem. Sci.* **23**, 68–73.
5. Hartl, F. U. & Hayer-Hartl, M. (2002). Molecular chaperones in the cytosol: from nascent chain to folded protein. *Science*, **295**, 1852–1858.
6. Mayer, M. P. & Bukau, B. (1998). Hsp70 chaperone systems: diversity of cellular functions and mechanism of action. *Biol. Chem.* **379**, 261–268.
7. Flaherty, K. M., DeLuca-Flaherty, C. & McKay, D. B. (1990). Three-dimensional structure of the ATPase fragment of a 70 K heat-shock cognate protein. *Nature*, **346**, 623–628.
8. Harrison, C. J., Hayer-Hartl, M., Di Liberto, M., Hartl, F. U. & Kuriyan, J. (1997). Crystal-structure of the nucleotide exchange factor GrpE bound to the ATPase domain of the molecular chaperone DnaK. *Science*, **276**, 431–435.
9. Zhu, X., Zhao, X., Burkholder, W. F., Gragerov, A., Ogata, C. M., Gottesman, M. E. & Hendrickson, W. A. (1996). Structural analysis of substrate binding by the molecular chaperone DnaK. *Science*, **272**, 1606–1614.
10. Morshauser, R. C., Wang, H., Flynn, G. C. & Zuiderweg, E. R. P. (1995). The peptide-binding

domain of the chaperone protein HSC70 has an unusual secondary structure topology. *Biochemistry*, **34**, 6261–6266.
11. Wang, H., Kurochkin, A. V., Pang, Y., Hu, W. D., Flynn, G. C. & Zuiderweg, E. R. P. (1998). NMR solution structure of the 21 kDa chaperone protein DnaK substrate binding domain: a preview of chaperone–protein interaction. *Biochemistry*, **37**, 7929–7940.
12. Bertelsen, E. B., Zhou, H. J., Lowry, D. F., Flynn, G. C. & Dahlquist, F. W. (1999). Topology and dynamics of the 10 kDa C-terminal domain of DnaK in solution. *Protein Sci.* **8**, 343–354.
13. Hendrick, J. P. & Hartl, F. U. (1993). Molecular chaperone functions of heat-shock proteins. *Annu. Rev. Biochem.* **62**, 349–384.
14. Gragerov, A., Li, Z., Xun, Z., Burkholder, W. & Gottesman, M. E. (1994). Specificity of DnaK peptide binding. *J. Mol. Biol.* **235**, 848–854.
15. Rüdiger, S., Germeroth, L., Schneider-Mergener, J. & Bukau, B. (1997). Substrate specificity of the DnaK chaperone determined by screening cellulose-bound peptide libraries. *EMBO J.* **16**, 1501–1507.
16. Flynn, G. C., Pohl, J., Flocco, M. T. & Rothman, J. E. (1991). Peptide-binding specificity of the molecular chaperone BiP. *Nature*, **353**, 726–730.
17. Pierpaoli, E. V., Sandmeier, E., Baici, A., Schönfeld, H.-J., Gisler, S. & Christen, P. (1997). The power stroke of the DnaK/DnaJ/GrpE molecular chaperone system. *J. Mol. Biol.* **269**, 757–768.
18. Palleros, D. R., Reid, K. L., Shi, L., Welch, W. J. & Fink, A. L. (1993). ATP-induced protein-Hsp70 complex dissociation requires K+ but not ATP hydrolysis. *Nature*, **365**, 664–666.
19. Schmid, D., Baici, A., Gehring, H. & Christen, P. (1994). Kinetics of molecular chaperone action. *Science*, **263**, 971–973.
20. McCarty, J. S., Buchberger, A., Reinstein, J. & Bukau, B. (1995). The role of ATP in the functional cycle of the DnaK chaperone system. *J. Mol. Biol.* **249**, 126–137.
21. Takeda, S. & McKay, D. B. (1996). Kinetics of peptide binding to the bovine 70 kDa heat shock cognate protein, a molecular chaperone. *Biochemistry*, **35**, 4636–4644.
22. Mayer, M. P., Schröder, H., Rüdiger, S., Paal, K., Laufen, T. & Bukau, B. (2000). Multistep mechanism of substrate binding determines chaperone activity of Hsp70. *Nature Struct. Biol.* **7**, 586–593.
23. Szabo, A., Langer, T., Schröder, H., Flanagan, J., Bukau, B. & Hartl, F. U. (1994). The ATP hydrolysis-dependent reaction cycle of the *Escherichia coli* Hsp70 system DnaK, DnaJ, and GrpE. *Proc. Natl Acad. Sci. USA*, **91**, 10345–10349.
24. Hartl, F. U. (1996). Molecular chaperones in cellular protein folding. *Nature*, **381**, 571–579.
25. Liberek, K., Marszalek, J., Ang, D., Georgopoulos, C. & Zylicz, M. (1991). *Escherichia coli* DnaJ and GrpE heat shock proteins jointly stimulate ATPase activity of DnaK. *Proc. Natl Acad. Sci. USA*, **88**, 2874–2878.
26. Russell, R., Karzai, A. W., Mehl, A. F. & McMacken, R. (1999). DnaJ dramatically stimulates ATP hydrolysis by DnaK: insight into targeting of Hsp70 proteins to polypeptide substrates. *Biochemistry*, **38**, 4165–4176.
27. Laufen, T., Mayer, M. P., Beisel, C., Klostermeier, D., Mogk, A., Reinstein, J. & Bukau, B. (1999). Mechanism of regulation of Hsp70 chaperones by DnaJ cochaperones. *Proc. Natl Acad. Sci. USA*, **96**, 5452–5457.
28. Packschies, L., Theyssen, H., Buchberger, A., Bukau, B., Goody, R. S. & Reinstein, J. (1997). GrpE accelerates nucleotide exchange of the molecular chaperone DnaK with an associative displacement mechanism. *Biochemistry*, **36**, 3417–3422.
29. Flynn, G. C., Chappell, T. G. & Rothman, J. E. (1989). Peptide binding and release by proteins implicated as catalysts of protein assembly. *Science*, **245**, 385–390.
30. Buchberger, A., Theyssen, H., Schröder, H., McCarty, J. S., Virgallita, G., Milkereit, P. *et al*. (1995). Nucleotide-induced conformational changes in the ATPase and substrate binding domains of the DnaK chaperone provide evidence for interdomain communication. *J. Biol. Chem.* **270**, 16903–16910.
31. Sadis, S. & Hightower, L. E. (1992). Unfolded proteins stimulate molecular chaperone Hsc70 ATPase by accelerating ADP/ATP exchange. *Biochemistry*, **31**, 9406–9412.
32. Blond-Elguindi, S., Fourie, A. M., Sambrook, J. F. & Gething, M. J. (1993). Peptide-dependent stimulation of the ATPase activity of the molecular chaperone BiP is the result of conversion of oligomers to active monomers. *J. Biol. Chem.* **268**, 12730–12735.
33. Slepenkov, S. V. & Witt, S. N. (1998). Peptide-induced conformational changes in the molecular chaperone DnaK. *Biochemistry*, **37**, 16749–16756.
34. Jordan, R. & McMacken, R. (1995). Modulation of the ATPase activity of the molecular chaperone DnaK by peptides and the DnaJ and GrpE heat shock proteins. *J. Biol. Chem.* **270**, 4563–4569.
35. Ha, J.-H. & McKay, D. B. (1995). Kinetics of nucleotide-induced changes in the tryptophan fluorescence of the molecular chaperone Hsc70 and its subfragments suggest the ATP-induced conformational change follows initial ATP binding. *Biochemistry*, **34**, 11635–11644.
36. Theyssen, H., Schuster, H. P., Packschies, L., Bukau, B. & Reinstein, J. (1996). The second step of ATP binding to DnaK induces peptide release. *J. Mol. Biol.* **263**, 657–670.
37. Russell, R., Jordan, R. & McMacken, R. (1998). Kinetic characterization of the ATPase cycle of the DnaK molecular chaperone. *Biochemistry*, **37**, 596–607.
38. Lorimer, G. (1997). Protein folding: folding with a two-stroke motor. *Nature*, **388**, 720–723.
39. Shtilerman, M., Lorimer, G. H. & Englander, S. W. (1999). Chaperonin function: folding by forced unfolding. *Science*, **284**, 822–825.
40. Gisler, S. M., Pierpaoli, E. V. & Christen, P. (1998). Catapult mechanism renders the chaperone action of Hsp70 Unidirectional. *J. Mol. Biol.* **279**, 833–840.
41. Hubbell, W. L. & Altenbach, C. (1994). In *Membrane Protein Structure* (White, S. H., ed.), pp. 224–228, Oxford University Press, New York.
42. Hubbell, W. L., Mchaourab, H. S., Altenbach, C. & Lietzow, M. A. (1996). Watching proteins move using site-directed spin labeling. *Structure*, **4**, 779–783.
43. Steinhoff, H. J., Mollaaghababa, R., Altenbach, C., Hideg, K., Krebs, M., Khorana, H. G. & Hubbell, W. L. (1994). Time-resolved detection of structural-changes during the photocycle of spin-labeled bacteriorhodopsin. *Science*, **266**, 105–107.
44. Steinhoff, H. J. (2004). Inter- and intra-molecular distances determined by EPR spectroscopy and site-directed spin labeling reveal protein–protein and protein–oligonucleotide interaction. *Biol. Chem.* **385**, 913–920.
45. Steinhoff, H. J. (2002). Methods for study of protein

dynamics and protein–protein interaction in protein-ubiquitination by electron paramagnetic resonance spectroscopy. *Front Biosci.* **7**, c97–c110.
46. Gragerov, A., Li, Z., Xun, Z., Burkholder, W. & Gottesman, M. E. (1994). Specificity of Dnak peptide binding. *J. Mol. Biol.* **235**, 848–854.
47. Feix, J. B. & Klug, C. S. (1998). Site-directed spin labeling of membrane proteins and peptide–membrane interactions. In *Biological Magnetic Resonance, Volume 14: Spin Labelling: The Next Millennium* (Berliner, L. J., ed.), pp. 251–281, Plenum Press, New York.
48. Buchberger, A., Valencia, A., McMacken, R., Sander, C. & Bukau, B. (1994). The chaperone function of DnaK requires the coupling of ATPase activity with substrate binding through residue E171. *EMBO J.* **13**, 1687–1695.
49. Steinhoff, H. J., Lieutenant, K. & Schlitter, J. (1989). Residual motion of hemoglobin-bound spin labels as a probe for protein dynamics. *Zeitschrift fur Naturforschung C-A J Biosci*, **44**, 280–288.
50. Steinhoff, H. J., Dombrowsky, O., Karin, C. & Schneiderhahn, C. (1991). Two dimensional diffusion of small molecules on protein surfaces: an EPR study of the restricted translational diffusion of protein-bound spin labels. *Eur. Biophys. J.* **20**, 293–303.
51. Likhtenstein, G. I. (1976). *Spin Labeling Methods in Molecular Biology*, Wiley, New York.
52. Steinhoff, H. J., Radzwill, N., Thevis, W., Lenz, V., Brandenburg, D., Antson, A. *et al*. (1997). Determination of interspin distances between spin labels attached to insulin: comparison of electron paramagnetic resonance data with the X-ray structure. *Biophys. J.* **73**, 3287–3298.
53. Rabenstein, M. D. & Shin, Y. K. (1995). Determination of the distance between 2 spin labels attached to a macromolecule. *Proc. Natl Acad. Sci. USA*, **92**, 8239–8243.
54. Radzwill, N., Gerwert, K. & Steinhoff, H. J. (2001). Time-resolved detection of transient movement of helices F and G in doubly spin-labeled bacteriorhodopsin. *Biophys. J.* **80**, 2856–2866.
55. Closs, G. L., Forbes, M. D. E. & Piotrowiak, P. (1992). Spin and reaction dynamics in flexible polymethylene biradicals as studied by EPR, NMR, and optical spectroscopy and magnetic-field effects—measurements and mechanisms of scalar electron-spin spin coupling. *J. Am. Chem. Soc.* **114**, 3285–3294.
56. Freed, J. H. (1976). Theory of slow tumbling ESR spectra for nitroxides. In *Spin Labelling. Theory and Applications* (Berliner, L. J., ed.), pp. 64–155, Academic Press, New York.
57. Misselwitz, B., Staeck, O. & Rapoport, T. A. (1998). J proteins catalytically activate Hsp70 molecules to trap a wide range of peptide sequences. *Mol. Cell*, **2**, 593–603.
58. McCarty, J. S., Rüdiger, S., Schönfeld, H.-J., Schneider-Mergener, J., Nakahigashi, K., Yura, T. & Bukau, B. (1996). Regulatory region c of the *E. coli* heat shock transcription factor, σ^{32}, constitutes a DnaK binding site and is conserved among Eubacteria. *J. Mol. Biol.* **256**, 829–837.
59. Slepenkov, S. V. & Witt, S. N. (2002). The unfolding story of the *Escherichia coli* Hsp70 DnaK: is DnaK a holdase or an unfoldase? *Mol. Microbiol.* **45**, 1197–1206.
60. Rothman, J. E. (1989). Polypeptide chain binding proteins: catalysts of protein folding and related processes in cells. *Cell*, **59**, 591–601.
61. Rothman, J. E. & Kornberg, R. D. (1986). Cell biology. An unfolding story of protein translocation. *Nature*, **322**, 209–210.
62. Hubbard, T. J. P. & Sander, C. (1991). The role of heat-shock and chaperone proteins in protein folding: possible molecular mechanisms. *Protein Eng.* **4**, 711–717.
63. Landry, S. J., Jordan, R., McMacken, R. & Gierasch, L. M. (1992). Different conformations for the same polypeptide bound to chaperones DnaK and GroEL. *Nature*, **355**, 455–457.
64. Stevens, S. Y., Cai, S., Pellecchia, M. & Zuiderweg, E. R. (2003). The solution structure of the bacterial HSP70 chaperone protein domain DnaK(393–507) in complex with the peptide NRLLLTG. *Protein Sci.* **12**, 2588–2596.
65. Moro, F., Fernandez, V. & Muga, A. (2003). Interdomain interaction through helices A and B of DnaK peptide binding domain. *FEBS Letters*, **533**, 119–123.
66. Buczynski, G., Slepenkov, S. V., Sehorn, M. G. & Witt, S. N. (2001). Characterization of a lidless form of the molecular chaperone DnaK. Deletion of the lid increases peptide on- and off-rate constants. *J. Biol. Chem.* **276**, 27231–27236.
67. Pellecchia, M., Montgomery, D. L., Stevens, S. Y., Vander Kooi, C. W., Feng, H. P., Gierasch, L. M. & Zuiderweg, E. R. P. (2000). Structural insights into substrate binding by the molecular chaperone DnaK. *Nature Struct. Biol.* **7**, 298–303.
68. Burkholder, W. F., Zhao, X., Zhu, X., Hendrickson, W. A., Gragerov, A. & Gottesman, M. E. (1996). Mutations in the C-terminal fragment of DnaK affecting peptide binding. *Proc. Natl Acad. Sci. USA*, **93**, 10632–10637.
69. Voisine, C., Craig, E. A., Zufall, N., von Ahsen, O., Pfanner, N. & Voos, W. (1999). The protein import motor of mitochondria: unfolding and trapping of preproteins are distinct and separable functions of matrix Hsp70. *Cell*, **97**, 565–574.
70. Montgomery, D. L., Morimoto, R. I. & Gierasch, L. M. (1999). Mutations in the Substrate BDdomain of the *Escherichia coli* 70 kDa molecular chaperone, DnaK, which alter substrate affinity or interdomain coupling. *J. Mol. Biol.* **286**, 915–932.
71. Palleros, D. R., Reid, K. L., McCarty, J. S., Walker, G. C. & Fink, A. L. (1992). DnaK, hsp73, and their molten globules. Two different ways heat shock proteins respond to heat. *J. Biol. Chem.* **267**, 5279–5285.
72. Shi, L., Kataoka, M. & Fink, A. L. (1996). Conformational characterization of DnaK and its complexes by small-angle X-ray scattering. *Biochemistry*, **35**, 3297–3308.
73. Wilbanks, S. M., Chen, L. L., Tsuruta, H., Hodgson, K. O. & McKay, D. B. (1995). Solution small-angle X-ray-scattering study of the molecular chaperone Hsc70 and its subfragments. *Biochemistry*, **34**, 12095–12106.
74. Slepenkov, S. V., Patchen, B., Peterson, K. M. & Witt, S. N. (2003). Importance of the D and E helices of the molecular chaperone DnaK for ATP binding and substrate release. *Biochemistry*, **42**, 5867–5876.
75. Ehresmann, B., Imbault, P. & Weil, J. H. (1973). Spectrophotometric determination of protein concentration in cell extracts containing tRNA's and rRNA's. *Anal. Biochem.* **54**, 454–463.
76. Merrifield, R. B. (1963). Solid phase peptide synthesis. 1. Synthesis of a tetrapeptide. *J. Am. Chem. Soc.* **85**, 2149–2153.
77. Schnolzer, M., Alewood, P., Jones, A., Alewood, D. &

Kent, S. B. H. (1992). *In situ* neutralization in boc-chemistry solid-phase peptide-synthesis—rapid. High-yield assembly of difficult sequences. *Int. J. Pept. Protein Res.* **40**, 180–193.
78. Bergmeyer, H. U. (1962). In *Methoden der Enzymatischen Analyse* (Adam, H., ed.), pp. 573–577, Verlag Chemie, Weinheim.
79. Tiebel, B., Radzwill, N., Aung-Hilbrich, L. M., Helbl, V., Steinhoff, H. J. & Hillen, W. (1999). Domain motions accompanying Tet repressor induction defined by changes of interspin distances at selectively labeled sites. *J. Mol. Biol.* **290**, 229–240.
80. Wegener, C. & Savitsky, A. (2001). High-field EPR-detected shifts of magnetic tensor components of spin label side chains reveal protein conformational changes: the proton entrance channel of bacteriorhodopsin. *Appl. Magn. Reson.* **21**, 441–452.

Edited by F. Schmid

(Received 12 November 2004; received in revised form 4 February 2005; accepted 9 February 2005)